Laser and Particle Beams (2001), *19*, 99–103. Printed in the USA.

Charge-exchange collisions in interpenetrating laser-produced magnesium plasmas

S.S. HARILAL,[1] C.V. BINDHU,[1] V.P. SHEVELKO,[2] AND H.-J. KUNZE[1]

[1]Institut fuer Experimentalphysik V, Ruhr-Universitaet Bochum, Universitaetsstrasse 150, D-44780 Bochum, Germany
[2]P.N. Lebedev Physics Institute, Russian Academy of Sciences, Moscow 117924, Russia

(RECEIVED 2 October 2000; ACCEPTED 5 February 2001)

Abstract

Charge-exchange collisions are one of the effective pumping methods for soft X-ray lasers. Experiments are performed to investigate charge-exchange collisions between highly charged Mg ions in colliding laser-produced magnesium plasmas. Pinhole photography and XUV spectroscopy are used as diagnostic tools. Spectroscopic studies show selective population of $n = 3$ levels of Mg IX ions, which results in enhancement of respective line intensities. Theoretical calculations also give a large cross section as high as 10^{-15} cm^2 for these charge-exchange collisions when the relative velocities of the colliding ions are of the order of 10^7 cm s^{-1}. XUV pinhole pictures are taken in early stages, which give more insight into the expansion dynamics of the colliding magnesium plasmas.

1. INTRODUCTION

Several applications of laser-produced plasmas involve an experimental situation where plasmas collide. Laser-produced colliding plasmas find potentially attractive applications in the field of X-ray lasers, and they are of relevance for the design of inertial confinement fusion (ICF) hohlraums (Kunze *et al.*, 1994; Glenzer *et al.*, 1997). In addition to these applications, the interpenetration of two plasmas occurs in a number of other systems, such as in astrophysical plasmas, when a supernova explosion ejects plasma into the interstellar medium, and barium is released into the solar wind, or when a comet interacts with the solar wind. Despite considerable experimental and theoretical progress in the dynamics of single laser-produced plasmas, little attention has been paid to studying the nature and dynamics of laser-produced colliding plasmas. Moreover most of the colliding plasma experiments were carried out using high intensity lasers ($>10^{13}$ W cm^{-2}) (Wan *et al.*, 1997). Experiments with low intensity lasers are extremely valuable for elucidating underlying science. Previous experiments have incorporated a variety of beam-target configurations including dual beam and parallel planar targets (Bosch *et al.*, 1992), split beam and single planar target (Henc-Bartolic *et al.*, 1998), split beam and target slabs placed orthogonally (Ruhl *et al.*, 1997), and single beam and internally irradiated microtubes (Stockl & Tsakiris, 1991). In conjunction with experimental studies, numerical modeling has been able to reproduce observed features of the plasma, such as the temperature, density, and emissivity (Chenais-Popovics *et al.*, 1997).

When two streaming plasmas collide, various interactions can arise. These may be of a collisionless type, in which case collective plasma effects occur, or they are collision dominated. Depending upon collisionality of the plasmas, which in turn depends on temperature, density, and ionic charge, varying amounts of interpenetration are predicted. In this article we report the characteristics of colliding laser-produced magnesium plasmas studied using XUV photography and XUV spectroscopy. We specifically investigate the possibility for charge-exchange collisions between ions of a hot plasma and a cold plasma.

2. EXPERIMENTAL SETUP

A schematic diagram of the experimental setup is given in Figure 1. A pulse from a ruby laser (6 J, 15 ns) is split into two beams with different intensities by means of a movable glass wedge. Changing of the position of the wedge can vary the intensity ratio of the two beams. These two beams are focussed by a plano-convex lens with a focal length $f =$ 300 mm onto two magnesium slabs placed at 90° to each other (Fig. 1b) that are kept in a vacuum chamber. The target slabs are placed on a motorized linear mount so that fresh surface is presented to the laser for each shot. This prevents

Address correspondence and reprint requests to: H.-J. Kunze, Institut fuer Experimentalphysik V, Ruhr-Universitaet Bochum, Universitaetsstrasse 150, D-44780 Bochum, Germany. E-mail: kunze@ep5.ruhr-uni-bochum.de

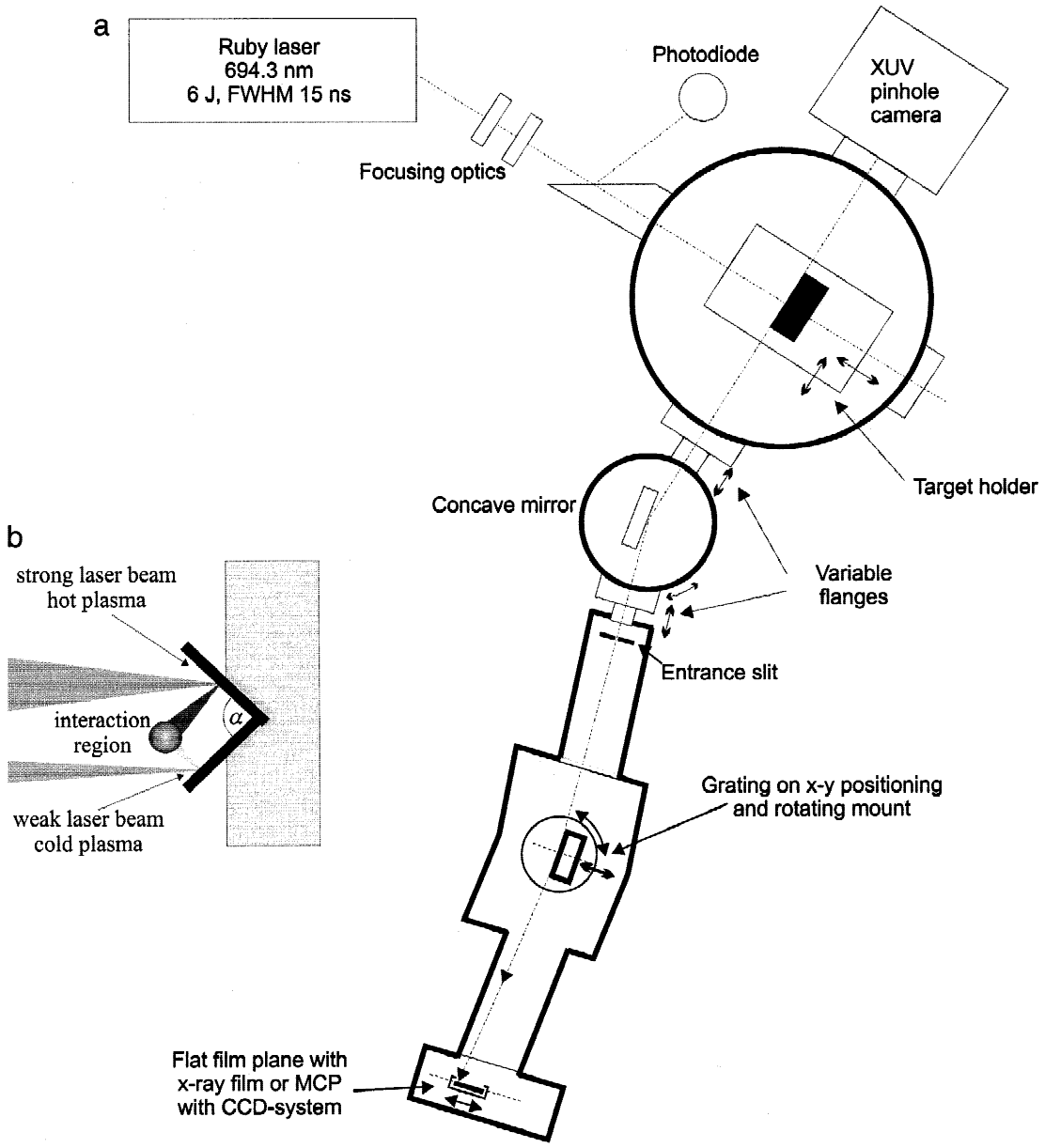

Fig. 1. (a) Schematic diagram of the experimental setup used for the XUV spectral studies. (b) Target geometry used for the present studies.

the creation of craters that will occlude emission from the hot core of the plasma. The distance between the two foci at the target surface is given by the relation $d = f\gamma(n-1)$, where $n = 1.5$, the refractive index and γ is the acute angle of the wedge. In the present studies we used a glass wedge with an acute angle of $17'02''$, which corresponds to a distance of separation between the foci of $d = 0.75$ mm. The estimated spot sizes on the target surface are approximately 400 μm. A gated (5 ns gate width) XUV pinhole camera is used to record two-dimensional time-resolved images of the colliding plasmas. For this we used a 50-μm pinhole with a microchannel plate combined with a charged-coupled device (CCD). The pinhole camera had an aluminum filter (27 mg cm^{-3}), resulting in a spectral sensitivity of the system of $<$80 nm. The pinhole pictures are taken from a direction perpendicular to the plane of the two laser beams. For spectral studies, a gold-coated spherical mirror with a 4-m radius of curvature is used to image the emitted radiation onto the entrance slit of the grazing incidence spectrograph. This setup essentially provides spatial resolution to better than 200 μm. The spectrograph is equipped with a concave grating set at an angle of incidence of 87°. The gold-plated grating with varying groove spacing focuses the spectrum on a flat plane instead of on the Roland circle. The spectrograph is coupled to a fast-gated flat microchannel plate with CCD camera.

3. RESULTS AND DISCUSSION

In the present experiment, the targets are mounted at an angle of 90° to each other. This arrangement leads to a good interpenetration of the two plasmas because of higher relative velocities than in the case of laterally colliding plasmas. The intensity ratio of two laser beams are made 7:1 that gives power densities $2\times10^{11}\,\mathrm{W\,cm^{-2}}$ and $3\times10^{10}\,\mathrm{W\,cm^{-2}}$, respectively. The positions of the foci of the hot and the cold plasma on the target surfaces are very important parameters because this governs the relative velocity with which the plasmas collide. To account for the higher expansion velocity of the hot plasma, the hot laser spot is placed closer to the common edge compared to the weak beam spot. A slight change in the geometry causes a drastic change in the shape and position of the interaction region.

Figure 2 gives pinhole pictures taken at different times after the maximum of the laser pulse. The bright plume in the lower part of the image is the hot plasma and the plume in the upper part is the cold plasma. For these studies, the MCP is gated at 5 ns. The expansion velocities of both plasmas are measured from the time evolution of the pinhole pictures. The estimated expansion velocities of hot and cold plasma in the initial stages are $(6\pm2)\times10^{6}\,\mathrm{cm\,s^{-1}}$ and $(3\pm1)\times10^{6}\,\mathrm{cm\,s^{-1}}$, respectively. Initially both plasmas expand freely. As time evolves, a thin interaction region begins to evolve at the collision region of the two plasmas and the intensity of the interaction region becomes brighter with time. It is interesting to note that the thickness of the interaction region becomes wider as time elapses. The length of the interaction region becomes ~1 mm (including penumbral image) at 15 ns after the laser maximum. At later times the collision region is found to be tilted towards the direction of the hot plasma (anticlockwise). The tilting of the collision region is expected to be due to the lower expansion velocity of the plasmas at the outer region of the target. At times greater than 25 ns, a radiating region appeared at the target slab close to the hot plasma. The high energetic ions and electrons from the hot plasma hit the target surface, which in turn creates a secondary plasma near the hot plasma.

The pinhole pictures suggest that the appearance of a jet starting in the collision region ~6 ns after the laser maximum. The spatial and temporal properties of this emission strongly depend on the laser power densities at the foci and the position of the spot from the point of contact of the target surfaces. The lifetime of the colliding plasma is found to be greater than the lifetime of the hot and cold plasmas. For sufficiently low plasma densities where the ion–ion mean free path exceeds the dimensions of the system, the two plasmas interpenetrate with little collisional interaction. Interpenetration of the plasmas takes place at short times (<1 ns), and during interpenetration the population density is perturbed by charge-exchange collisions. At high plasma densities, where the ion–ion mean free path is smaller than the plasma density scale lengths, the region of plasma interpenetrating is relatively small. In this case, plasma stagnates. Rancu *et al.* (1995), describing the experimental study of the collision of aluminum plasma with magnesium plasma, confirms that the plasmas interpenetrate each other at early times and stagnate at later times. When these plasmas collide, the directed kinetic energy can be converted into thermal energy; the plasmas heat up and slow down. The relative velocity of the plasmas will be reduced by the interaction and the momentum transfer cross sections increased. This in

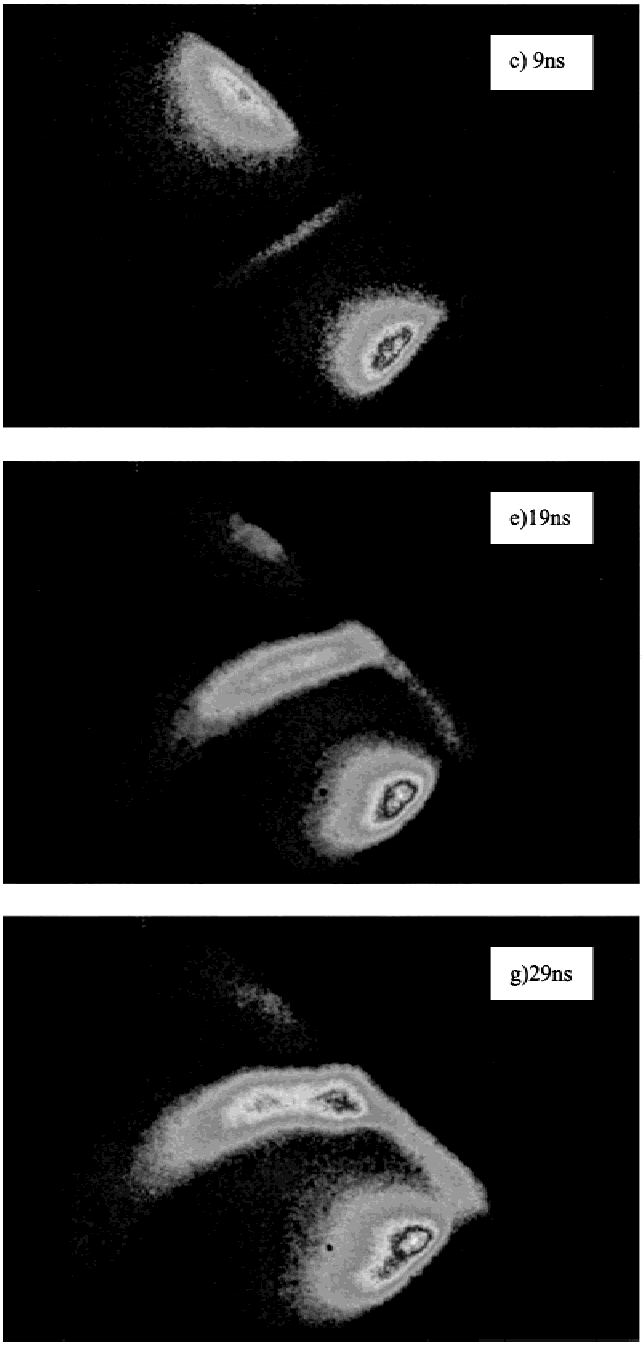

Fig. 2. Time evolution of colliding plasmas recorded using a 50-μm pinhole camera. The time given in the pictures is the delay of the gate pulse after the laser pulse maximum. The gate width was set at 5 ns.

turn will create a rapid build-up of stationary plasma in the interaction region having the appearance of a jet.

Spectroscopic studies are needed in the present case to find out whether the emission of the collision zone is due to stagnation of the plasmas or if the plasmas interpenetrate and show stronger emission due to charge-exchange collisions. XUV spectra are taken in the spectral range 3–8 nm using a grazing incidence spectrograph. Figure 3 gives such a spectrum for colliding plasmas. The spectrum was taken at a distance of 0.8 mm from the common edge of the targets and 8 ns after the maximum of the laser pulse. Spectrum of the hot plasma is also given in Figure 3 and serves as a reference. The MCP is gated for 10 ns for the spectral studies. Enhanced line emission and continuum emission is observed from the collision region.

The spectra of Figure 3 are dominated by emission due to Li-like (Mg X) and Be-like (Mg IX) magnesium ions. Figure 4 gives the intensity ratio of the prominent spectral lines observed for colliding plasmas normalized to the intensity emitted from the hot plasma alone after subtracting the continuum. We observed enhancement in line intensities for different ionic lines and it is predominant for lines originating from the $n = 3$ level for Be-like magnesium. The intensity enhancement for lines originating from $n \geq 4$ is less evident in the observed spectra. The selective population of the level $n = 3$ is attributed to charge-exchange collisions that take place between the magnesium ions. The electron-capture cross sections have been calculated for the following charge-exchange process:

$$\mathrm{MgX} + \mathrm{MgV} \rightarrow \mathrm{MgIX} + \mathrm{MgVI}. \quad (1)$$

Cross sections as high as 10^{-15} cm^{-2} are obtained for lines originating from $n = 3$ levels for the relative velocities of the $\sim 10^7$ cm s^{-1} (Shevelko, 2000; Tolstikhina & Shevelko, 2000). The calculated cross sections for lines originating from other n levels are several orders of magnitude less in the desired relative velocity range. This leads to the selective population of the $n = 3$ levels of Be-like ions and thus accounts for the enhancement of the intensity of lines originated in these levels compared to other high-lying levels ($n \geq 4$). It is also noted that the intensity growth for these lines is prominent in the early stages. So we expect that at the beginning of the collision, the plasmas interpenetrate and afterwards stagnate.

4. CONCLUSIONS

We investigated the possibility for charge-exchange collisions between Li-like magnesium ions in a hot plasma and Mg V ions in a cold plasma. Theoretical estimations lead to selective population of $n = 3$ levels of Be-like magnesium ions. The spectroscopic observation averages over a cross

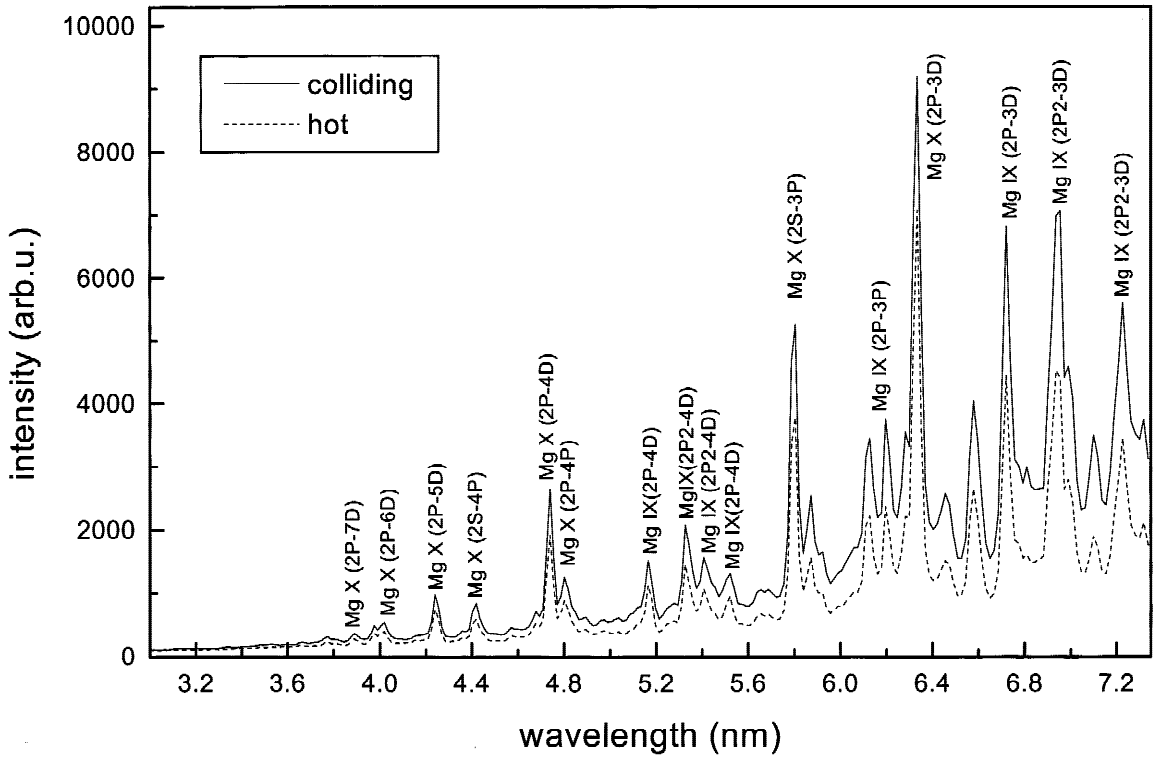

Fig. 3. Spectrum of colliding and hot plasmas. They were recorded at a distance of 0.8 mm from the common edge of the targets and by setting the gate width at 10 ns.

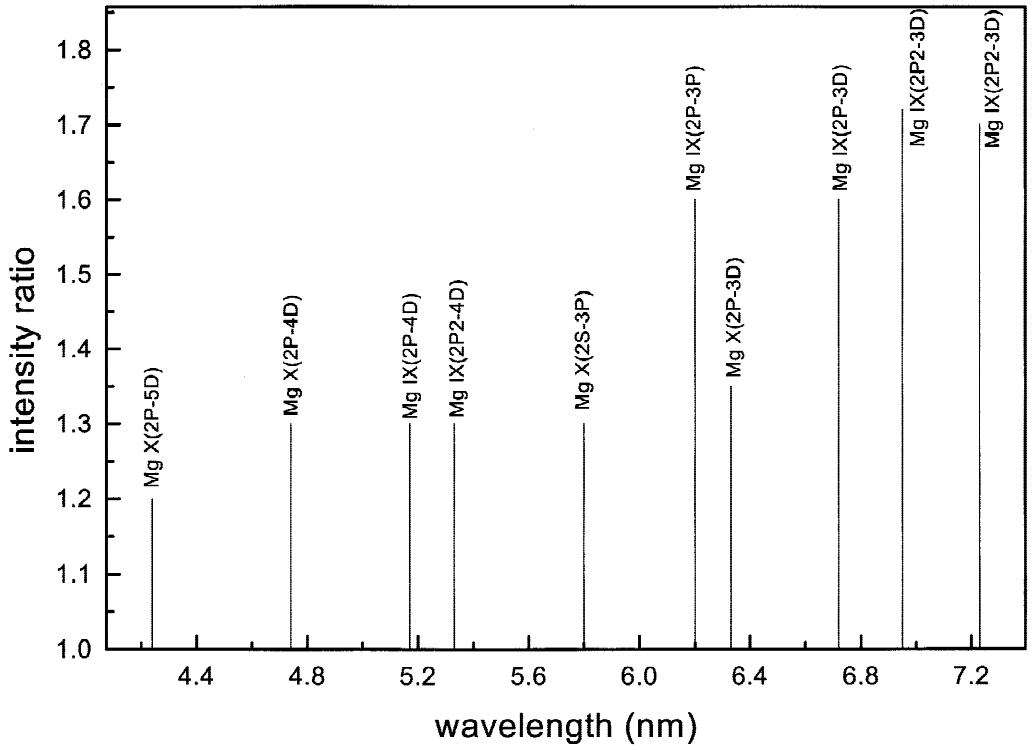

Fig. 4. Intensity ratio of lines from colliding plasma with lines from hot plasma.

section of the expanding plasmas larger than the interaction region. So the true local enhancement of the lines thus certainly will be even larger than recorded. Moreover the time resolution of the present experiment is not fully adequate to study the dynamics of charge-exchange collisions. Time-resolved photographic studies of colliding laser-produced magnesium plasma give more insight into the expansion dynamics of the collision region.

ACKNOWLEDGMENTS

SSH thanks the Alexander von Humboldt Foundation, Germany, for a research fellowship.

REFERENCES

Bosch, R.A. *et al.* (1992). *Phys. Fluids B* **4**, 979.
Chenais-Popovics, C. *et al.* (1997). *Phys. Plasmas* **4**, 190.
Glenzer, S.H. *et al.* (1997). *Phys. Rev. Lett.* **79**, 1277.
Henc-Bartolic, V. *et al.* (1998). *Phys. Scripta* **T75**, 297.
Kunze, H.J. *et al.* (1994). *Phys. Lett. A* **193**, 183.
Rancu, O. *et al.* (1995). *Phys. Rev. Lett.* **75**, 3854.
Ruhl, F. *et al.* (1997). *Phys. Lett. A* **225**, 107.
Shevelko, V.P. (2000). *GSI Rep. 2000-1*, 115.
Stockl, C. & Tsakiris, G.D. (1991). *Laser Part. Beams* **9**, 725.
Tolstikhina, Y. & Shevelko, V.P. (2000). *Short Commun. Phys.* (Moscow), **5**, 46.
Wan, A.S. *et al.* (1997). *Phys. Rev. E* **55**, 6923.